Anomalous decay of multilayer holes on $SrTiO_3(001)$

Mahito Yamamoto,[1,*] Koichi Sudoh,[1] Hiroshi Iwasaki,[1] and Ellen D. Williams[2]
[1]*The Institute of Scientific and Industrial Research, Osaka University, 8-1 Mihogaoka, Ibaraki, Osaka 567-0047, Japan*
[2]*Department of Physics, Material Research Science and Engineering Center, Center for Nanophysics and Advanced Material, University of Maryland, College Park, Maryland 20742-4111, USA*
(Received 3 July 2010; published 20 September 2010)

The decay behavior of nanoscale multilayer holes on $SrTiO_3(001)$ has been studied using scanning tunneling microscopy. The multilayer hole shrinks rigidly keeping steps in bunches, which is followed by rapid decay of a bottom single or a few layers in the hole at a critical volume. Both the critical volume and the number of layers exhibiting the rapid decay increase with depth of the hole. We have found that the anomalous morphological evolution during decay is induced as a result of the competition between the curvature effect and the short-range attractive step interaction. The attractive interaction gives rise to metastable step configurations of the bunching in the hole. Then the metastable state vanishes at the critical volume due to the enhanced curvature effect with decrease in size, which causes the debunching of the steps. The presented experimental results combined with a numerical simulation based on a step-flow model allowing for attractive step interactions have revealed that the depth of the step interaction potential well on $SrTiO_3(001)$ is approximately 4.6 ± 2.0 meV.

DOI: 10.1103/PhysRevB.82.115436 PACS number(s): 05.70.Np, 68.35.Md, 68.37.Ef

I. INTRODUCTION

Fundamental understanding of thermal instability and associated morphological evolution of nanostructures on crystalline surfaces has been of increasing importance toward a practical use of electronic nanodevices. The nanostructure on the surface is, in general, thermodynamically unstable and diminishes with time in a complicated way, depending on surface energetic and kinetic parameters correlated with constitutive material system. In order to obtain comprehensive knowledge of the behaviors of the nanostructures in nonequilibrium, thus, experimental investigations on each target material are necessary. Even in such an essential complexity the intrinsic decay behaviors of the nanostructures on various surfaces are known to be universally described by a few surface parameters.[1–5] For example, the collapses of the mounds are understood in terms of the motion of atomic steps, which are driven by mass transport between the steps. The mass transport occurs along the gradient of step chemical potentials typically consisting of the step line tension and the step interaction energy.[6,7] In previous interpretations on the decay of the three-dimensional islands, the predominant interactions considered are an elastic dipole interaction or an entropic interaction, which lead to repulsion between the steps at a long range.[1–4,8–10]

In this paper we experimentally show a class of decay behaviors of the nanoscale multilayer hole significantly governed by an attractive step interaction. The multilayer hole on an oxide of $SrTiO_3(001)$ shrinks, keeping respective step-step distances almost constant, which is followed by abrupt split-off of a single layer or a few layers at the bottom in the hole at specific volumes. The critical volume increases with increasing the depth of the hole. The number of the bottom detaching layers shows an increasing trend with the depth as well. The observed decay behaviors are manifestly different from well-known layer-by-layer or pairwise layer relaxations reported previously.[1–5] We elucidate the anomalous morphological evolution by introducing a short-range attractive interaction between the nearest-neighboring steps. The attractive step interaction plays a role in the formation of metastable step configurations of the bunching during decay. However with decrease in size, the steps in bunches become thermodynamically unstable because of the enhanced curvature effect, resulting in the rapid decay of a single or a few bottom layers at a critical volume. We have performed numerical simulations based on a step-flow model allowing for a simple model step interaction. The simulation results reproduce well the distinct observations, that is, the step bunching and the subsequent debunching during decay.

II. EXPERIMENTAL

The sample was cut from a Nb-doped $SrTiO_3(001)$ substrate and cleaned by sonication in acetone. Then we introduced the sample into an ultrahigh vacuum (UHV) chamber with a base pressure of 1.0×10^{-8} Pa equipped with a variable temperature scanning tunneling microscopy (STM). In UHV the sample was annealed at 700–800 °C for a few hours using a resistive heater, which resulted in a flat surface with steps with one-unit-cell height of 0.4 nm, implying that the surface was terminated with either TiO_2 or SrO. The sample temperature was measured by a pyrometer. The fabrications of the nanoscale holes on the $SrTiO_3(001)$ surface and the observations of the decay processes of the holes were conducted using STM at 750 °C. To minimize the effects of the thermal drift on the STM images, the STM tip was initially located several tens of micrometers away from the surface heated at 750 °C and held for a few hours before the observations. After the thermal drift decreased to about 50 nm/h, we fabricated the multilayer holes by applying a bias voltage of 5–10 V from the STM tip on the $SrTiO_3(001)$ surface and subsequently imaged the decay of the holes in constant current mode at resolution of 512×512 pixels. The scan rate was 0.5–1 μm/s. Within the range of the scan rate

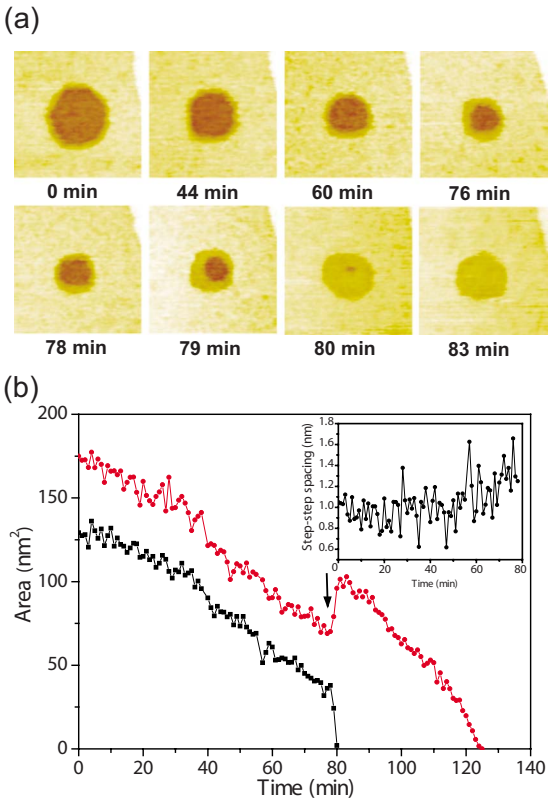

FIG. 1. (Color online) (a) STM images (30 nm × 30 nm) of the decay of the double hole and (b) the time evolution of the area of each layer and the step-step spacing. When the volume of the hole decreases down to 43 nm^3 at 79 min as indicated by the arrow, the bottom layer rapidly decays while the upper layer expands.

the holes were not disrupted by the STM tip during imaging. The areas of the innermost and the outermost layers of the multilayer holes were measured for each image.

Figure 1(a) is a sequence of STM images of a double-layer hole on $SrTiO_3(001)$ at 750 °C. Figure 1(b) illustrates time evolution of the area of each layer and the step-step spacing in the hole shown in Fig. 1(a). The hole, with initial volume of 122 nm^3 and the step-step spacing of about 1.0 nm, decays at a rate of 0.98 nm^3/min. For the first 78 min, the upper and the lower layer diminish at mean decay rates of 1.4 and 1.2 nm^2/min, keeping the step-step distance nearly constant with slight increase as shown in the inset of Fig. 1(b). We observe rapid decay of the bottom layer, of which rate increases by a factor of 18, when the volume goes down to 43 nm^3 and the step-step spacing broadens to 1.2 nm at 79 min. Simultaneously the top layer expands at the same rate as the bottom layer until the bottom layer is completely filled. During the rapid decay the mass is locally conserved between the two layers. The series of the decay events are repeatedly observed. From 16 observations for the double-layer holes at around 750 °C we find the rapid decay is invariably ignited when the volume of the hole goes down to about 32 nm^3.

The multilayer hole exhibits more complicated decay features. As an example a morphological evolution of a six-layer hole at 750 °C is shown in Fig. 2. Initially the volume is 652 nm^3 and the spacing between the outermost and the innermost layer is 3.9 nm, which yields 0.8 nm as an average spacing between the adjacent steps. The areas of the outermost and the innermost layer are plotted as a function of time in Fig. 3. The hole contracts keeping the steps in bunches at a mean decay rate of 0.54 nm^2/min for the outermost layer and 0.45 nm^2/min for the innermost layer until the volume of the hole decreases down to 454 nm^3 at 137 min. Afterward the inner double layer abruptly decays at a mean rate of 10 nm^2/min, which is followed by the rapid decay of the innermost layer when the volume of the inner subhole goes down to 34 nm^3 at 143 min shown in Fig. 2. The volume is consistent with the critical volume obtained for the isolated double-layer hole. Consecutively we observe the two rapid decay events of the innermost single layer at the volume of 168 nm^3 and 83 nm^3, respectively.

We observe similar decay behaviors, i.e., the step bunch formation with a step-step spacing of 1.0 ± 0.2 nm and the following debunching at critical volumes for a various depths of the holes. The repeated observations of decay of the multilayer holes reveal that the critical volume monotonically increases with increasing depth of the hole as shown in Fig. 4. Also the number of the rapidly decaying layers shows an increasing trend with depth. The histogram in Fig. 4 illustrates the number of layers which exhibit the rapid decay for each depth of the hole. For six- to ten-layer holes the fast decay of the triple layer is consistently observed.

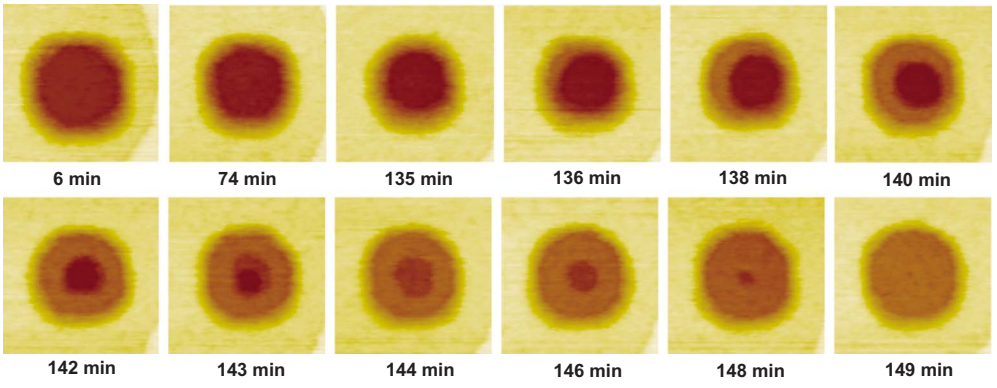

FIG. 2. (Color online) STM images (30 nm × 30 nm) of decay of the six-layer hole. At 136 min the bottom double layer abruptly decays and subsequently the rapid decay of the innermost layer occurs in the subhole at 143 min.

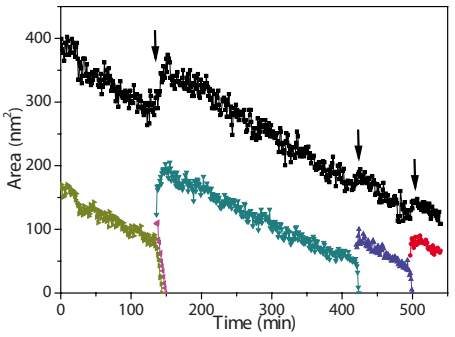

FIG. 3. (Color online) The time evolution of the areas of the outermost layer and the innermost layer of the hole shown in Fig. 2. The hole eventually decays into the double-layer hole after the fast decay events at 137, 420, and 497 min as indicated by the arrows. The critical volumes are 454 nm^3, 168 nm^3, and 83 nm^3, respectively.

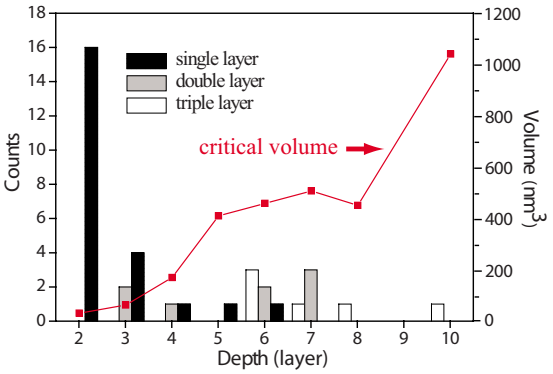

FIG. 4. (Color online) The averaged critical volume as a function of the depth of the hole and the histogram for the number of the fast decaying layers for each depth of the hole. The black, gray, and white bars indicate the rapid decay of the single, double, and triple layer at the critical volume.

III. DISCUSSION

The decay processes of the layered structures are, simply speaking, controlled by an interplay between thermodynamical driving forces such as the step line tension and the step-step interactions, the rate limiting processes, and the step permeability. In the surface-diffusion limited process, the complete disappearance of the innermost layer triggers the rapid decay of the next layer, which results in layer-by-layer decay.[3,11] In this case the step kinetics are quite fast and thus the permeable steps may not influence the layer-by-layer decay process. On the other hand, in the kinetics limited process, the highly permeable steps give rise to simultaneous decay of the layers such as pairwise layer decay.[1,4]

The previous studies on the decay of the holes on $SrTiO_3(001)$ reveal that the steps are impermeable and the decay rate is limited by the surface diffusion at around 750 °C.[11,12] In the present observations we find the mass is locally conserved during the rapid decay as shown in Fig. 1, indicating the step-permeating mass flow is small likely due to the barely permeable steps as reported previously.[11] Also after 81 min the single-layer hole decays with time following $(t_c-t)^{\alpha}$ power law with $\alpha=0.71$, where t_c is disappearance time, which suggests that the decay is limited by surface diffusion.[13] Despite the combined condition of the diffusion limited process and the impermeability of the step, however, the present observations for the decay of the hole are manifestly different from the layer-by-layer decay. All layers decay maintaining the respective step-step spacings nearly constant until the rapid decay occurs. Furthermore the rapid decay of the bottom single, double, or triple layer is triggered by critical sizes that rigorously depend on the depth of the hole.

The existence of the critical sizes as shown in Fig. 4 suggests that the morphological feature is not due to a kinetic effect but an energetic reason. Thus we propose that the step bunching above the critical volume is a metastable structure of the hole for each volume. In the diffusion limited process a system of steps can reach a metastable equilibrium state for each volume since the step kinetics are much faster than the interstep surface diffusion. The local minimum in the step free energy may be accounted for by a presence of an attractive step interaction. The attractive interactions between adjacent steps have been experimentally observed on various surfaces.[14,15] Especially on $SrTiO_3(001)$, a short-range attractive step interaction has been reported.[16] The attractive step interaction supposedly acts at a step-step spacing in the range of 1–2 nm since the hole with each initial step-step spacing of greater than 2 nm decays mostly by layer-by-layer disappearance due to a long-range repulsive interaction.[11]

Some theoretical explanations have been proposed for the attractive step interaction.[17–21] However the exact physical origin of the attractive step interaction on $SrTiO_3(001)$ has remained vague. Therefore in order to model the experimental results quantitatively, we assume that the attractive step interaction can be approximately described by a high-order term of the surface free energy density expanded by a power series of the step density ρ (Refs. 17 and 22)

$$f(\rho) = f_0 + f_1\rho + f_2\rho^2 + f_3\rho^3 + f_4\rho^4 + \cdots, \tag{1}$$

where f_0 is the surface free energy density of the flat surface, $f_1\rho$ is the step free energy density, and $f_i\rho^i$ $(i \geq 2)$ are the contributions of the step interaction energies. Among them especially f_3 indicates the elastic or the entropic repulsive interaction. The surface free energy density can be rewritten in terms of the step-step spacing l (Ref. 23)

$$f(l) = f_0 + \frac{\beta}{l} + \frac{f_2h^2}{l^2} + \frac{f_3h^3}{l^3} + \frac{f_4h^4}{l^4} + \cdots, \tag{2}$$

where β is the step free energy and h is the height of the step. Following the representations by Degawa *et al.*,[23–25] the total step free energy $F(r_1, r_2, \ldots, r_N)$ of an N-layer hole is given by

$$F(r_1, r_2, \ldots, r_N) = \sum_{i=1}^{N-1} \pi(r_{i+1}^2 - r_i^2)(f(l_i) - f_0), \tag{3}$$

where r_i $(r_{i+1} > r_i)$ is the radius of the ith layer and $l_i = r_{i+1} - r_i$ is the step-step spacing between the ith layer and the $i+1$th layer. We define the step-step interaction $U(l_i)$ that is a

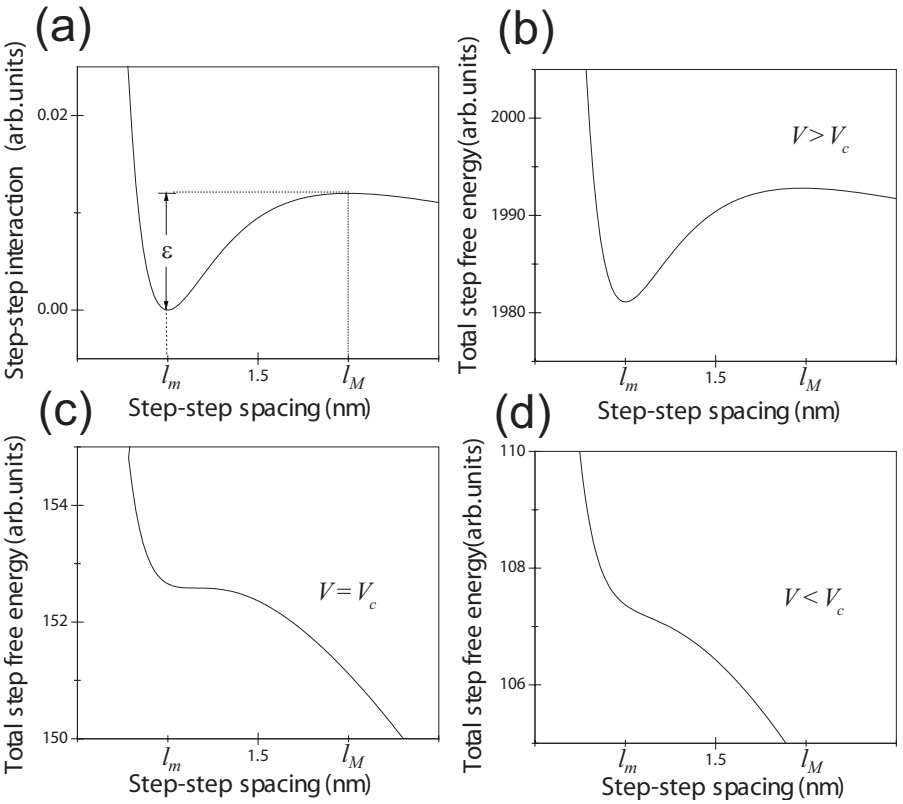

FIG. 5. (a) The model step-step interaction, which has a local minimum at $l=l_m$ and a local maximum at $l=l_M$. The depth of the potential well is ϵ. Here we choose $l_m=1.0$ nm, $l_M=2.0$ nm, and $\epsilon=0.012\beta$. [(b)–(d)] The total step free energy for various volume calculated by using the step interaction shown in (a). (b) At $V > V_c$ there exists a local minimum point at around $l=1.0$ nm. (c) At $V_c=68$ nm^3 the local minimum point disappears. (d) Below V_c, the double step becomes totally unstable throughout the step-step spacing.

linear combination of the power of the inverse step-step spacing as

$$U(l_i) = \frac{f_2 h^2}{l_i} + \frac{f_3 h^3}{l_i^2} + \frac{f_4 h^4}{l_i^3} + \frac{f_5 h^5}{l_i^4} + \cdots . \tag{4}$$

Here let f_4, which is likely of a dipole-quadrupole interaction origin,[26] be the attractive step interaction and f_5 be the repulsive step interaction in order to prevent the total step interaction from diverging to a negative infinite energy as l_i goes to 0. The other short-range interaction terms are ruled out. Additionally the long-range interaction $f_2 h^2/l_i$ likely due to the quantum effects implicated in surface states is commonly negligible.[27] Equation (4) reduces to

$$U(l_i) = \frac{f_3 h^3}{l_i^2} + \frac{f_4 h^4}{l_i^3} + \frac{f_5 h^5}{l_i^4} \tag{5}$$

with f_3, $f_5 > 0$ and $f_4 < 0$. We should note that the choice of the power here is not based on the physical origin of the step interaction on $SrTiO_3(001)$ but just for the sake of convenience. Using Eq. (5) the total step free energy of Eq. (3) is rewritten to

$$F(r_1, r_2, \ldots, r_N) = \sum_{i=1}^{N} 2\pi r_i \beta + \sum_{i=1}^{N-1} \pi (r_{i+1} + r_i) U(l_i). \tag{6}$$

First, we focus on the double-layer hole for simplicity. The total step free energy of the double-layer hole is

$$F(r_1, r_2) = 2\pi (r_1 + r_2)\beta + \pi (r_1 + r_2) U(l), \tag{7}$$

where $l=r_2-r_1$. This free energy can be expressed by the hole volume $V=\pi h(r_1^2+r_2^2)$ and the step-step spacing l as

$$F(l, V) = \pi \sqrt{\frac{2V}{\pi h} - l^2}\,[2\beta + U(l)]. \tag{8}$$

As will be shown later in Appendix, we can rewrite the interaction parameters in Eq. (5) in terms of the experimentally accessible parameters ϵ, l_m, and l_M, where ϵ is the depth of the potential well and l_m and l_M give the local minimum and maximum of the potential, respectively. Figure 5(a) illustrates a model step-step interaction characterized by ϵ, l_m, and l_M. The interaction parameters l_m and l_M here are set to 1.0 and 2.0 nm to suit to the experimental observations. On the other hand at present there is no quantitative information on the potential well ϵ. Thus we provisionally adopt the depth of the potential well $\epsilon=0.012\beta$ as will be determined later by comparing the experimental observations with simulation results. Using the same parameters the step free energy for various volumes as a function of the spacing l are shown in Figs. 5(b)–5(d). For larger volume [Fig. 5(b)], there exists a local minimum point around $l=l_m$ due to the attractive step interaction, which gives rise to a metastable configuration in the double step. However as seen in Fig. 5(c), the local minimum point disappears as the volume of the hole decreases down to $V_c=68$ nm^3. Eventually below V_c [Fig. 5(d)] the double-layer hole falls into a thermodynamically unstable state.

In order to elucidate the origin of the induced instability of the hole with decrease in volume, we focus on the behavior of the step-step spacing at a metastable state for each volume. The metastable step-step spacing can be derived from the chemical potentials of the steps. Using Eq. (6), we define the step chemical potential of the ith step as

$$\mu_i = -\frac{\Omega}{2\pi r_i}\frac{\partial F(r_1, r_2, \ldots)}{\partial r_i} = -\frac{\Omega\beta}{r_i} - \frac{\Omega}{2r_i}[U(l_i) + U(l_{i-1})] + \frac{\Omega}{2r_i}[(r_i + r_{i+1})U'(l_i) - (r_{i-1} + r_i)U'(l_{i-1})], \quad (9)$$

where Ω is the area occupied by an atom and $U'(l_i)$ represents $dU(l_i)/dl_i$.[8,9] In Eq. (9) the first term indicates Gibbs-Thomson effect, the second term is due to the step interaction associated with the curvature radius, and the third term is also the step interaction term in the thermodynamic limit.[23] If the neighboring steps lie at a local equilibrium state, the chemical potentials of the steps are equivalent. Here we define the chemical potential differences between the adjacent steps as

$$\Delta\mu_{i+1,i} = \mu_{i+1} - \mu_i = -\Omega\beta\left(\frac{1}{r_{i+1}} - \frac{1}{r_i}\right) - \frac{\Omega}{2}\left[\frac{U(l_{i+1}) + U(l_i)}{r_{i+1}} - \frac{U(l_i) + U(l_{i-1})}{r_i}\right] + \frac{\Omega}{2}\left[\frac{(r_{i+1} + r_{i+2})U'(l_{i+1}) - (r_i + r_{i+1})U'(l_i)}{r_{i+1}} - \frac{(r_i + r_{i+1})U'(l_i) - (r_{i-1} + r_i)U'(l_{i-1})}{r_i}\right]. \quad (10)$$

The first and the second curvature-related terms are possibly cancelled out by the last step interaction term in the metastable state. Initially we specifically view the step chemical potential difference of the double-layer hole, which is given by

$$\Delta\mu_{2,1} = -\Omega\beta\left(\frac{1}{r_2} - \frac{1}{r_1}\right) - \frac{\Omega U(l)}{2}\left(\frac{1}{r_2} - \frac{1}{r_1}\right) - \frac{\Omega(r_1 + r_2)U'(l)}{2}\left(\frac{1}{r_2} + \frac{1}{r_1}\right). \quad (11)$$

In the large volume limit, the metastable state is secured at $l = l_m$ where $U'(l_m) = 0$ as seen in Fig. 5(b). With decrease in volume, the metastable step-step spacing gently broadens for the attractive force $U'(l)$ to compensate the curvature effect. Figure 6(a) illustrates the step-step spacing l as a function of the volume at the metastable state obtained by numerically solving $\Delta\mu_{2,1} = 0$ for each volume. Here we use the same interaction parameters for $U(l)$ as used in Fig. 5. The metastable spacing between the steps widens with decrease in volume and eventually disappears when the volume decreases down to 68 nm^3. This behavior of the step-step spacing is consistent with the experimental results shown in the inset of Fig. 1(b). At the critical volume the metastable spacing reaches to 1.14 nm, where the attractive force $U'(l)$ is nearly the maximum value. The fact implies that there is no longer enough spacing for the attractive force to balance out the curvature effect. Thus at $l > l_c = 1.14$ nm, due to the curvature effect the chemical potential difference becomes always positive, which leads to mass flows from the upper layer into the lower layer.

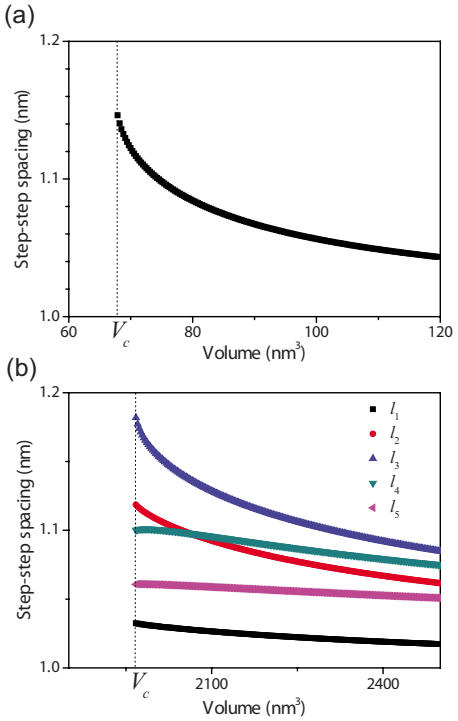

FIG. 6. (Color online) The step-step spacing as a function of volume at a metastable state for (a) the double-layer hole and (b) the six-layer hole. At the critical volume, the metastable step-step spacing disappears. In (b) The third step-step spacing is wider than any other spacings, which results in the split-off of the bottom triple layer.

Next we apply the analogy to analysis of the $N(>2)$-layer hole. As with the double-layer hole, from Eq. (10) the curvature effect is negligible at large volume and the free energy has the local minimum points at $l_1 = l_2 = \cdots = l_{N-1} = l_m$ which gives the local minimum of the step interaction $U(l_i)$. With decreasing volume the curvature effects may invoke the disappearance of the metastable state. We search for the local minimum points in the total step free energy of the six-layer hole around $l_i = l_m$ $(i = 1, 2, \ldots, 5)$ by numerically solving the simultaneous equations, $\Delta\mu_{i+1,i} = 0$ $(i = 1, 2, \ldots, 5)$ for each volume. Figure 6(b) is a plot of the metastable step-step spacing as a function of volume. The interaction parameters are the same as used in the analysis of the double-layer hole, that is, $\epsilon = 0.012\beta$, $l_m = 1.0$ nm, and $l_M = 2.0$ nm. With decreasing volume the respective step-step spacings gradually broaden due to the curvature effect. Especially l_3 is notably wider than any other step-step spacings while the lowermost and the uppermost step-step spacing, l_1 and l_5 are relatively small. Then, when the l_3 reaches to 1.18 nm at $V = 1967$ nm^3, the local minimum points around $l_i = l_m$ disappear and the chemical potential difference between the third and the fourth step is produced. The chemical potential gradient induces the mass exchange between the third layer and the fourth layer and the subsequent detachment of the lower triple layer.

In an analogous way, by solving the simultaneous equations, $\Delta\mu_{i+1,i} = 0$ $(i = 1, 2, \ldots, N-1)$ for each volume, we examine the critical volume and the number of the detaching layers as a function of the depth of the hole, N. Figure 7 is a

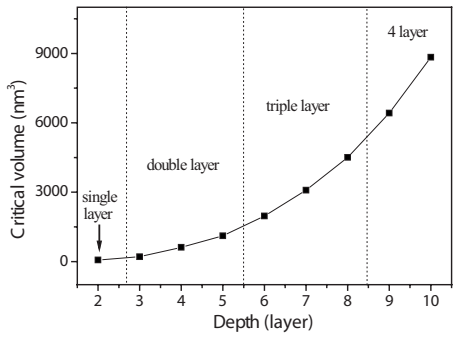

FIG. 7. The critical volume as a function of the depth of the hole obtained by numerically solving $\Delta\mu_{i+1,i}=0$ for each volume. The number of the detaching layers for each depth are also shown. The dotted lines in the graph indicate the boundaries at which the number of the detaching layers changes.

plot of the critical volume as a function of the depth of the hole. The critical volume monotonically increases with increase in depth, which is consistent with the experimental observations. The increase in the critical volume can be understood by simply comparing the curvature effects of holes with different depths but equivalent volume and step density. In this case the radius of each layer in the deeper hole is smaller than that of the corresponding layer in the shallower hole. Thus the deeper hole is more influenced by the curvature effects than the shallower hole if they have same volume and as a result the critical volume increases with depth.

Figure 7 also shows the number of the detaching layers. The debunching is induced nearly at the middle of the hole or at a layer lower than the middle layer in the range of 2–10 layer. Namely, taking a broad view, the detaching layer also increases with depth, qualitatively agreeing with the observations.

The numerically obtained critical volume and the number of the detaching layers qualitatively well reproduce the experimental results shown in Fig. 4 but are overestimated. The overestimations can be corrected considering kinetic effects of decay as will be discussed in the following section.

Thus far we have assumed the short-range step interaction takes the form of a linear combination of the power of the inverse spacing, $1/l$ for simplicity. Then in order to generalize the arguments, we shed light on the condition for the step interactions under which the structural instability is induced at a certain volume without specifying the power for the step interaction in Eq. (4). We simply assume the depth of the potential well ϵ at the step-step spacing, l_m and the effective length of the attraction, l_M as illustrated in Fig. 5(a). Focusing on the double-layer hole, the critical point of the stable-unstable transition in morphology coincides to a saddle point of the total step free energy Eq. (8), that is, $\partial F/\partial l|_{V_c,l_c}=0$ and $\partial^2 F/\partial l^2|_{V_c,l_c}=0$, where V_c is the critical volume and l_c is the critical step-step spacing. These yield simultaneous equations for the critical volume and the critical spacing in terms of $U(l_c)$, $U'(l_c)=dU(l)/dl|_{l=l_c}$, and $U''(l_c)=d^2U(l)/dl^2|_{l=l_c}$

$$\left(\frac{2V_c}{\pi h}-l_c^2\right)U'(l_c)-l_c[2\beta+U(l_c)]=0 \tag{12}$$

and

$$\left(\frac{2V_c}{\pi h}-l_c^2\right)U''(l_c)-[2\beta+U(l_c)+3l_cU'(l_c)]=0. \tag{13}$$

The condition for the step interaction, under which the structural instability is induced at a finite volume is given by $V_c > \pi h l_c^2/2$. Accordingly we get a condition, $2\beta+U(l_c)>0$ with $l_m<l_c<l_{inf}<l_M$, where l_{inf} is the inflection point of the $U(l)$. From this condition, we find if $2\beta+U(l_{inf})<0$, the disappearance of the metastable state can not be observed since the steps are strongly trapped by the potential well.

IV. NUMERICAL SIMULATIONS

Up to this point we have addressed the observed morphological transition during decay in terms of energetics. In the actual nonequilibrium system, however, the critical phenomenon is supposed to be susceptible to the kinetics of decay. To verify validity of our discussion proposed in the previous section in a dynamical system, where the mass transport is limited by the diffusion, we perform numerical simulations using a step-flow model allowing for a model step interaction Eq. (5) transcribed in terms of ϵ, l_m, and l_M. Once again we should emphasize that the representation of the step interaction adopted here does not reflect a physical origin of the step interaction on $SrTiO_3(001)$.

The rate of change in the radius of the ith step is given by

$$\frac{dr_i}{dt}=-\frac{\Omega c_0 D_s}{k_B T r_i}\left[\frac{\mu_{i+1}-\mu_i}{\ln(r_{i+1}/r_i)}-\frac{\mu_i-\mu_{i-1}}{\ln(r_i/r_{i-1})}\right], \tag{14}$$

where D_s is the diffusion coefficient and c_0 is the equilibrium adatom concentration.[8–10] Here we assume that the concentration at the outside of the hole equilibrates at $r=R_e$ as a boundary condition. The boundary condition determines the decay rate in the simulation. Figure 8 shows the simulation results for the time evolution of the area of each layer for (a) the double-layer and (b) the six-layer hole using Eq. (14) with the same interaction parameters as used in the previous analysis, that is, $\epsilon=0.012\beta$, $l_m=1.0$ nm, and $l_M=2.0$ nm. For the boundary condition we choose $R_e=25$ nm to suit the experimental results shown in Fig. 1. Time axes in the simulation results are rescaled by a factor, $k_BT/(\Omega^{1/2}\beta D_s c_0)$ of 1.45 s obtained by comparison of the decay rate with the experimental value of 0.98 nm^3/min. In Fig. 8(a) we see the rapid decay of the first layer accompanying the expansion of the second layer at $V=43$ nm^3, which both qualitatively and quantitatively reproduces the experimental observations. Likewise Fig. 8(b) shows a series of the abrupt decay of the bottom double layers at $V=905$ nm^3 and 340 nm^3, representing good qualitative agreement with the experimental results shown in Fig. 3. The discrepancy in the number of the layers that rapidly decay for the four-layer hole may be due to the variability of the experimental observations resulting from different boundary conditions.

To see the kinetic effects on the critical phenomena in the morphological evolution, we additionally conduct the simulations for various depths of the hole employing two different boundary conditions, the decay rates of 0.56 and 1.0 nm^3/min. The critical volume as a function of the hole depth is shown in Fig. 9. For both decay rates the critical

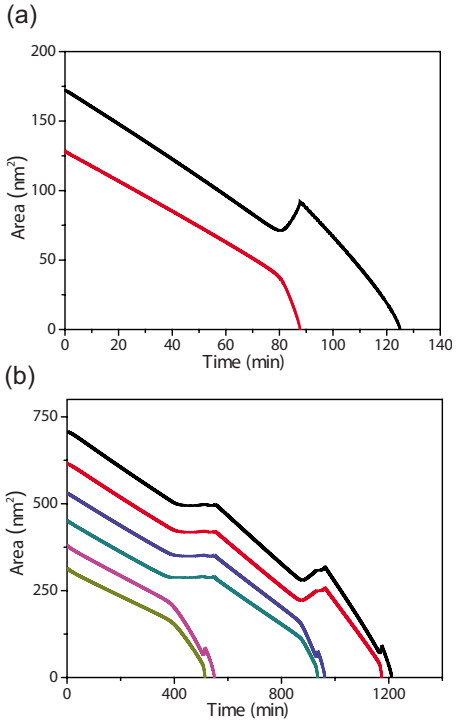

FIG. 8. (Color online) The numerical simulation results of the time evolution of the area of each layer for (a) the double-layer and (b) the six-layer hole. The interaction parameters are $\epsilon=0.012\beta$, $l_m=1.0$ nm, and $l_M=2.0$ nm.

volume for every depth and the number of the fast decaying layers for some depth are smaller than the results in the static state shown in Fig. 7. For the shallower hole the critical volume is less affected by the external mass flow. However the critical volume and the fast decaying layers for the lower decay rate increasingly become larger than for the faster decay rate with depth. Hence we find in the dynamical system the rapid mass flux from the upper step into the lower step is suppressed by the external mass flowing into the hole and thus the step-step spacing remains less than the critical value even at the critical volume found in the static state, which leads to decrease in the critical volume. By fitting the simulation results to the experimental results for the double-layer

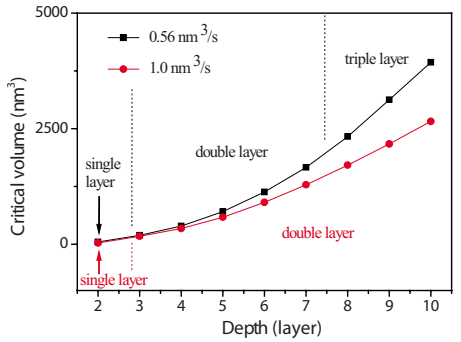

FIG. 9. (Color online) The numerical simulation results of the critical volume as a function of the depth of the hole for two decay rates of 0.56 and 1.0 nm^3/min. The number of layers which shows the rapid decay for each depth is also shown.

hole, we quantitatively obtain the depth of the potential well ϵ of $(0.012\pm0.005)\beta$. Using the step free energy on $SrTiO_3(001)$ of $\beta=382\pm6$ meV at 700–750 °C,[28] the depth of the potential well is roughly determined to be 4.6 ± 2.0 meV.

Whereas the simulation results reproduce well the distinctive aspects in the experimental observations shown in Fig. 4, there are discrepancies in the critical layers between the simulation and the experimental results for some depth of the hole. This is likely due to not only external mass flow but also thermal fluctuations of the steps in the experiments. The step fluctuation induces the incidental broadening of a step-step spacing more than the effective attraction distance. Indeed large step fluctuations are experimentally observed. Even if the stochastic events including the change in the external mass flow during decay are not taken into account in our simulations, the remaining robust consistency between the simulation and the experimental results manifests that our interpretations on the anomalous decay behavior are reasonable.

V. SUMMARY

We have observed the anomalous morphological evolution of the multilayer holes on $SrTiO_3(001)$ surfaces by using STM. Initially the multilayer hole decays while maintaining the steps in bunches. Subsequently the rapid decay events occur at a critical volume which depends on the depth of the hole. Also the critical layers which show the rapid decay increase with increase in depth. We conclude that the hole decays via metastable states produced by the attractive step-step interaction. Furthermore the enhanced curvature effect with decrease in size induces the disappearance of the metastable state which results in the rapid decay of the bottom single layer or the multilayer. The experimentally observed increases of the critical volume and the critical layer are explained in terms of the competition between the curvature effect and the short-range attractive interaction between the adjacent steps. We have performed numerical simulations based on the step-flow model, which allows for the attractive step interaction described by minimal parameters. As a result we have obtained the approximate depth of the step interaction potential well of 4.6 ± 2.0 meV.

ACKNOWLEDGMENTS

We would like to thank Y. Yamada and K. Burson for fruitful discussions.

APPENDIX

We transform the interaction parameters, f_3, f_4, and f_5 in Eq. (5) into the obvious expressions of ϵ, l_m, and l_M by solving the simultaneous equations, $U'(l_M)=0$, $U'(l_m)=0$, and $\epsilon=U(l_M)-U(l_m)$ for ϵ, l_m, and l_M as follows:

$$f_3h^3=\frac{6(l_ml_M)^3}{(l_M-l_m)^3(l_m+l_M)}\epsilon, \tag{A1}$$

$$f_4 h^4 = -\frac{4(l_m l_M)^3}{(l_M - l_m)^3}\epsilon, \tag{A2}$$

$$f_5 h^5 = \frac{3(l_m l_M)^4}{(l_M - l_m)^3 (l_m + l_M)}\epsilon. \tag{A3}$$

*Present address: Department of Physics, University of Maryland, College Park, MD 20742-4111, USA.

[1] S. Tanaka, N. C. Bartelt, C. C. Umbach, R. M. Tromp, and J. M. Blakely, Phys. Rev. Lett. **78**, 3342 (1997).
[2] A. Ichimiya, K. Hayashi, E. D. Williams, T. L. Einstein, M. Uwaha, and K. Watanabe, Phys. Rev. Lett. **84**, 3662 (2000).
[3] K. Thürmer, J. E. Reutt-Robey, E. D. Williams, M. Uwaha, A. Emundts, and H. P. Bonzel, Phys. Rev. Lett. **87**, 186102 (2001).
[4] S. Kodambaka, N. Israeli, J. Bareño, W. Święch, K. Ohmori, I. Petrov, and J. E. Greene, Surf. Sci. **560**, 53 (2004).
[5] M. Giesen and H. Ibach, Surf. Sci. **431**, 109 (1999).
[6] H. C. Jeong and E. D. Williams, Surf. Sci. Rep. **34**, 171 (1999).
[7] M. Giesen, Prog. Surf. Sci. **68**, 1 (2001).
[8] M. Uwaha and K. Watanabe, J. Phys. Soc. Jpn. **69**, 497 (2000).
[9] N. Israeli and D. Kandel, Phys. Rev. B **60**, 5946 (1999).
[10] D. Margetis, M. J. Aziz, and H. A. Stone, Phys. Rev. B **71**, 165432 (2005).
[11] M. Yamamoto, K. Sudoh, and H. Iwasaki, Surf. Sci. **601**, 1255 (2007).
[12] H. Goto, K. Sudoh, and H. Iwasaki, e-J. Surf. Sci. Nanotechnol. **4**, 307 (2006).
[13] J. G. McLean, B. Krishnamachari, D. R. Peale, E. Chason, J. P. Sethna, and B. H. Cooper, Phys. Rev. B **55**, 1811 (1997).
[14] J. Frohn, M. Giesen, M. Poensgen, J. F. Wolf, and H. Ibach, Phys. Rev. Lett. **67**, 3543 (1991).
[15] K. Sudoh, T. Yoshinobu, H. Iwasaki, and E. D. Williams, Phys. Rev. Lett. **80**, 5152 (1998).
[16] K. Sudoh and H. Iwasaki, Surf. Sci. **557**, L151 (2004).
[17] C. Jayaprakash, C. Rottman, and W. F. Saam, Phys. Rev. B **30**, 6549 (1984).
[18] A. C. Redfield and A. Zangwill, Phys. Rev. B **46**, 4289 (1992).
[19] C. V. Ciobanu, D. T. Tambe, V. B. Shenoy, C. Z. Wang, and K. M. Ho, Phys. Rev. B **68**, 201302(R) (2003).
[20] R. V. Kukta, A. Peralta, and D. Kouris, Phys. Rev. Lett. **88**, 186102 (2002).
[21] G. Wang, J. F. Webb, and J. Zi, Surf. Sci. **601**, 1944 (2007).
[22] N. Cabrera and N. García, Phys. Rev. B **25**, 6057 (1982).
[23] M. Degawa, F. Szalma, and E. D. Williams, Surf. Sci. **583**, 126 (2005).
[24] M. Degawa and E. D. Williams, Surf. Sci. **595**, 87 (2005).
[25] M. Degawa, K. Thürmer, and E. D. Williams, Phys. Rev. B **74**, 155432 (2006).
[26] R. Najafabadi and D. J. Srolovitz, Surf. Sci. **317**, 221 (1994).
[27] N. García and P. A. Serena, Surf. Sci. **330**, L665 (1995).
[28] M. Yamamoto, M.Eng. thesis, Osaka University, 2008.